J Ind Microbiol Biotechnol (2008) 35:751–760
DOI 10.1007/s10295-008-0343-8

ORIGINAL PAPER

Microbe repelling coated stainless steel analysed by field emission scanning electron microscopy and physicochemical methods

Mari Raulio · Mikael Järn · Juhana Ahola · Jouko Peltonen · Jarl B. Rosenholm · Sanna Tervakangas · Jukka Kolehmainen · Timo Ruokolainen · Pekka Narko · Mirja Salkinoja-Salonen

Received: 14 September 2007 / Accepted: 11 March 2008 / Published online: 1 April 2008

Abstract Coating of stainless steel with diamond-like carbon or certain fluoropolymers reduced or almost eliminated adhesion and biofilm growth of *Staphylococcus epidermidis*, *Deinococcus geothermalis*, *Meiothermus silvanus* and *Pseudoxanthomonas taiwanensis.* These species are known to be pertinent biofilm formers on medical implants or in the wet-end of paper machines. Field emission scanning electron microscopic analysis showed that *Staph. epidermidis*, *D. geothermalis* and *M. silvanus* grew on stainless steel using thread-like organelles for adhesion and biofilm formation. The adhesion threads were fewer in number on fluoropolymer-coated steel than on plain steel and absent when the same strains were grown in liquid culture. *Psx. taiwanensis* adhered to the same surfaces by a mechanism involving cell ghosts on which the biofilm of live cells grew. Hydrophilic (diamond-like carbon) or hydrophobic (fluoropolymer) coatings reduced the adherence of the four test bacteria on different steels. Selected topographic parameters, including root-mean-square roughness (S_q), skewness (S_{sk}) and surface kurtosis (S_{ku}), were analysed by atomic force microscopy. The surfaces that best repelled microbial adhesion of the tested bacteria had higher skewness values than those only slightly repelling. Water contact angle, measured (θ_m) or roughness corrected (θ_y), affected the tendency for biofilm growth in a different manner for the four test bacteria.

Keywords Ultrastructure · Bacterial adhesion · Field emission scanning electron microscope (FESEM) · Physicochemical parameters · Contact angle · Topographic analysis

M. Raulio (✉) · J. Ahola · M. Salkinoja-Salonen
Department of Applied Chemistry and Microbiology, University of Helsinki, P. O. Box 56, 00014 Helsinki, Finland
e-mail: mari.raulio@helsinki.fi

M. Järn · J. Peltonen · J. B. Rosenholm
Department of Physical Chemistry, Åbo Akademi University, Porthaninkatu 3-5, 20500 Turku, Finland

S. Tervakangas · J. Kolehmainen
DIARC-Technology Inc, Olarinluoma 15, 02200 Espoo, Finland

T. Ruokolainen · P. Narko
Alu-Releco Oy, Kynttilätie 10, 11710 Riihimäki, Finland

Introduction

Biomass accumulated on industrial process surfaces may cause process failure, contamination and defects of end products [10]. Biofilm formation is also a frequent reason for failure of biomedical devices such as catheters, cardiac pacemakers, and prosthetic joints and causes infections [3, 5, 29].

Biomaterials impregnated with antimicrobial compounds, such as antibiotics [20, 32, 38], organics (triclosan, benzalkonium chloride) [14, 22, 28] or inorganics (silver and other heavy metals) [9, 13, 16, 31], have been intensively studied for medical applications. Antimicrobial chemicals have limited efficacy against biofilms [6] and the biocide usage may damage the environment, e.g., silver ions are cytotoxic and non-biodegradable; therefore, alternatives are needed.

One possibility is to engineer the technical surfaces so that microbes do not attach. With this as the aim, we investigated stainless steels with newly engineered coatings with no direct antimicrobial activity. As model organisms we used bacterial species known as formers of primary biofilms on steel equipment in warm water industry [17, 18, 37], or on medical devices (reviewed by Mack et al. 2006; Söderqvist 2007) [23, 34] to evaluate the

significance of selected physical parameters expressing surface quality. We show in this paper, novel ultrastructural features of the bacteria expressed when growing on coated and non-coated acid proof steel.

Materials and methods

Preparation of biofilms

The bacterial strains and conditions used are described in Table 1. To test biofilm growth, the steel coupons were cleaned and disinfected as described earlier [27]. The coupons were placed in wells of 12- or 6-well polystyrene plates in upright position, partially immersed in the test medium seeded with 5 vol% inoculate. Biofilms on the test coupons were stained with a nucleic acid-specific fluorochrome and the fluorescence translated into cfu units as described earlier [27].

Field emission scanning electron microscopy (FESEM)

Micrographs of the test coupons were prepared as described earlier [27]. Planktonic cultures were grown in broth (Table 1) for 1 day, centrifuged (5 min, 1,600 g), washed with autoclaved drinking water, fixed in phosphate (0.1 M, pH 7.2) buffered 2.5% glutaraldehyde for 2 h, and rinsed with the phosphate buffer three times. The fixed cells were dehydrated with an ethanol series (50, 75, 96, 100%), critical point dried (Bal-Tec CPD 030; Bal-Tec AG, Balzers, Liechtenstein) and mounted on SEM specimen stubs using graphite glue (Colloidal graphite, Electron Microscopy Sciences, Ft. Washington, PA, USA). The stubs were coated with Pt/Pb (10 nm, 208 HR High Resolution Sputter Coater, Cressington Scientific Instruments Inc., Cranberry, PA, USA) and examined with Hitachi S-4800 FESEM (Tokyo, Japan) operated at 1 kV.

Topographic analysis by atomic force microscopy (AFM) and image analysis

The images were recorded with a Nanoscope IIIa AFM (Digital Instruments, Santa Barbara, CA) in tapping mode using silicon cantilevers with a resonance frequency between 250 and 300 kHz. The scan rate was typically 0.7–2 Hz. The free tapping amplitude was 70–100 nm for the high-kinetic-energy tapping measurements. The damping ratio r_{sp} (=A_{sp}/A_0) controlling the level of forced damping was chosen by tuning the set-point amplitude, A_{sp}. All images (512 × 512 pixels) were measured in air without filtering. The microscope was placed on an active vibration isolation table (MOD-1M, JRS Scientific Instruments, Switzerland), which was further placed on a massive stone table to eliminate external vibrational noise. The scanning probe image processor (SPIP, Image Metrology, Denmark) software was used for the roughness analysis of the images [1].

The set of roughness parameters selected for this study was developed and standardized by Stout et al. [35] and expanded by Peltonen et al. [26] for versatile characterization of various surface properties in three dimensions. The reported roughness values in this study are mean values from up to ten images. The interpretation of the selected parameters is as follows: the root-mean-square (RMS) roughness S_q is the most widely used amplitude roughness parameter that actually gives the standard deviation of height. Surface skewness S_{sk} describes the asymmetry of the height distribution. A skewness value equal to 0 represents a Gaussian-like surface. Negative values of S_{sk} refer to a surface-porous sample, i.e., the valleys dominate over the peak regimes. In the same way, the local maxima dominate over the valleys for S_{sk} >0. Surface kurtosis S_{ku} gives a measure for the sharpness of the surface height distribution. A Gaussian value for this parameter is 3.0; much smaller values indicate a very broad (heterogeneous) height distribution, whereas values much larger than 3.0 refer to a surface with almost quantized height values. The number of local maxima per unit area is given by the spatial parameter S_{ds}. Besides the number also the form of the local maxima (summits) is of certain interest. Two hybrid parameters describe the form of the summits: the mean summit curvature, S_{sc}, and the RMS value of the surface slope, S_{dq}.

Most of the above parameters contribute to the effective surface area: the absolute height difference, the number and form of local maxima, among others. A measure for the change of effective surface area with respect to the projected

Table 1 Strains and conditions used for growing the biofilms

Strain	Growth conditions	Origin of the strain
D. geothermalis E50051	R2 broth, 45 °C	Paper machine [37]
M. silvanus BR2A5504	R2 broth, 45 °C	Wire section, paper machine [18]
Psx. taiwanensis JN11306	R2 broth, 45 °C	Paper machine [17]
Staph. epidermidis O47 PIA+	BHI broth, 37 °C	Medical implant [12]

The monoculture biofilms were grown for 2 days under rotation (160 rpm) from inoculate (5 vol%) grown in liquid medium for 1 day. *Staph. epidermidis* O47 (PIA+) was a gift from Friedrich Götz (University of Tübingen, Germany). The other strains were from the collection of M.S. Salkinoja-Salonen

Table 2 The acid proof steels used as base for coating

	Chemical composition wt%[a]							Used for
	C	Si	Cr	Mn	Fe	Ni	Mo	
Steel #1	1.8	1.7	16.6	1.6	66.3	10.2	2.6	As base for fluoropolymer coatings
Steel #2	1.8	0.5	16.5	1.1	67.3	10.3	2.9	As base for DLC coatings

[a] Determined by energy dispersive X-ray spectroscopy (EDS/EDX) analysis

area is given in percentages by the surface area ratio parameter S_{dr}. The S_{dr} parameter was used to calculate the r value ($r = 1 + S_{dr}/100$), which denotes the ratio between the real and the projected surface area of the sample. According to Wenzel [39] the relation between the roughness-dependent measured contact angle θ_m and Young's contact angle θ_y corresponding to an ideally flat surface may be written as $\cos \theta_m = r \cos \theta_y$. A more thorough description of the parameters was given in a recent paper [26].

Contact angle measurements

A CAM 200 contact angle goniometer (KSV Instruments Ltd., Helsinki, Finland) was used for determination of contact angles (θ_m). The contact angles of water on the solid substrates were measured in air. The contact angles were calculated using software delivered with the instrument. The size of the droplets was ~2 μm. The results are given as a mean from three to five measurements.

Preparing the coatings on steel

The steels used for coating were of acid proof quality (Table 2) with no polishing. Diamond like carbon (DLC-A and DLC-B) coatings were prepared on stainless steel AISI316L/2B (steel #2) by DIARC-Technology Inc. (Espoo, Finland) using DIARC® plasma coating method which is a technology for manufacturing hydrogen free amorphous diamond coatings. Coatings were deposited in vacuum at a temperature below 100 °C. The nanostructure of the coating

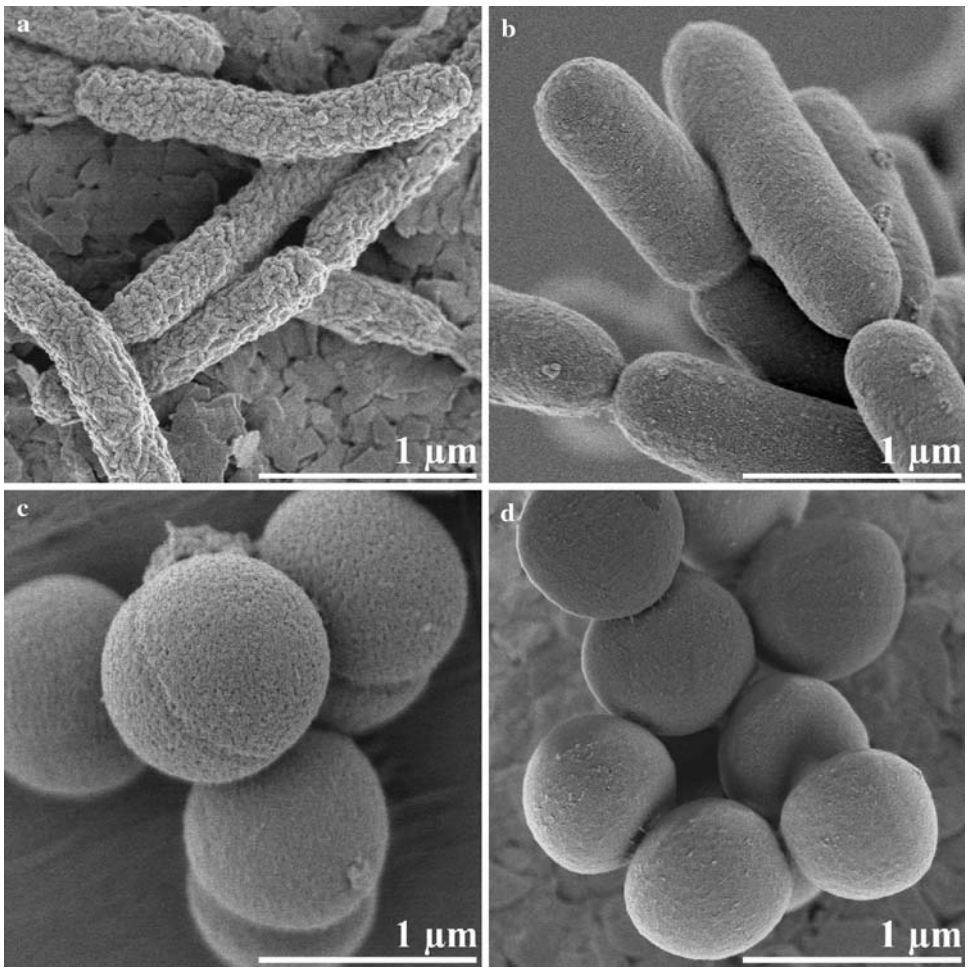

Fig. 1 FESEM micrograph of over night liquid culture of **a** *Psx. taiwanensis* JN 11306, **b** *M. silvanus* B-R2A5-50.4, **c** *D. geothermalis* E50051 and **d** *Staph. epidermidis* O-47 (PIA+). Putative adhesion threads, giant cells of *M. silvanus* (Fig. 3) or cell ghosts of *Psx. taiwanensis* (Fig. 2) were not seen in the liquid cultures of these bacteria

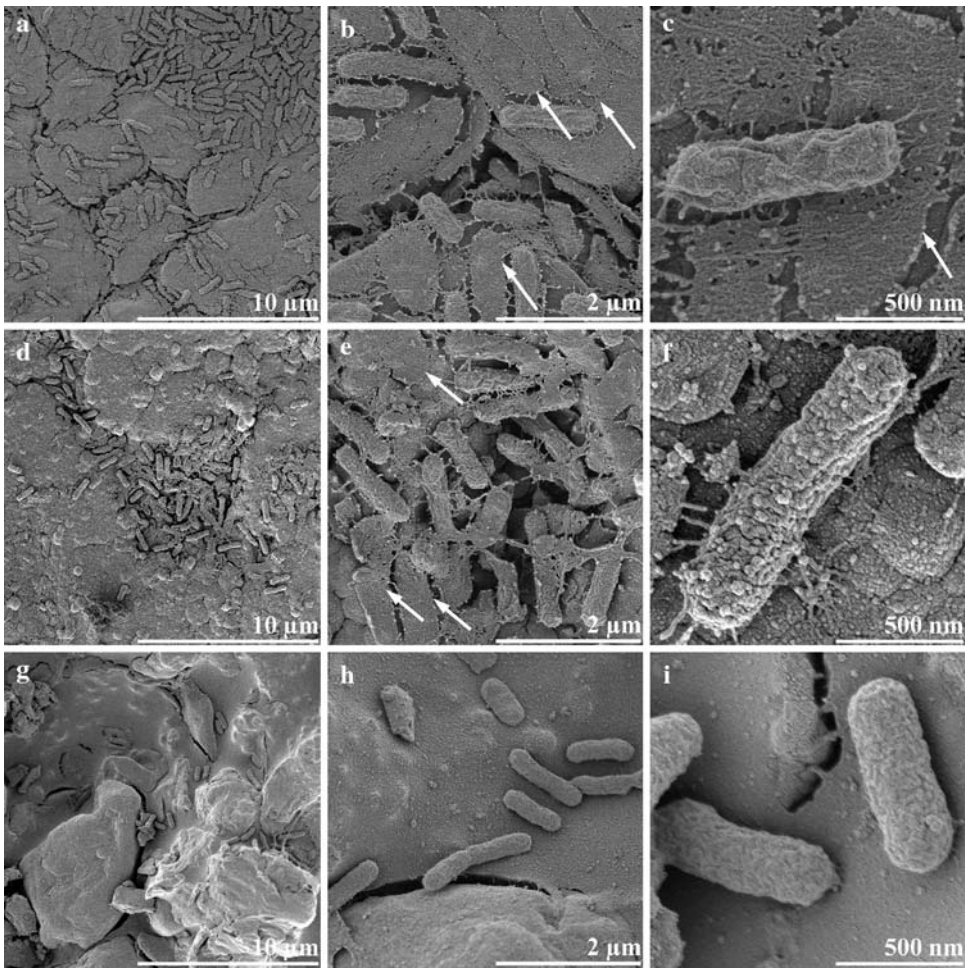

Fig. 2 FESEM micrographs of *Psx. taiwanensis* JN 11306 adhered to coated or non-coated stainless steel surfaces. **a–c** Non-coated stainless steel AISI316L/2B (steel #2, Table 2). **d–f** Diamond like carbon coating DLC-A on steel AISI316L/2B. **g–i** AR-115 fluoropolymer-coated acid-fast stainless steel #1. *Arrows* in **b**, **c** and **e** point at cell ghosts

was customized by varying the process parameters. Fluoropolymer coatings were prepared on acid proof stainless steel (steel #1) by Alu-Releco Oy (Riihimäki, Finland).

Chemicals and reagents

R2A [7] and brain hearth infusion (BHI) broth were purchased from Difco (Becton, Dickinson and Company Franklin Lakes, NJ, USA). Syto9 was from Molecular Probes (Leiden, The Netherlands) and hexamethyldisilazane from Fluka (Buchs, Switzerland).

Results

Growth of *Pseudoxanthomonas taiwanensis*, *Deinococcus geothermalis*, *Meiothermus silvanus* and *Staphylococcus epidermidis* (Table 1) on non-coated or coated stainless steels was investigated under high-flow conditions in laboratory media. Ultrastructures of liquid culture (Fig. 1) and surface-grown cells of these organisms were inspected by FESEM (Figs. 2, 3, 4, 5).

The biofilms of *Psx. taiwanensis* contained large amounts of cell ghosts and numerous short (<100 nm) appendages (Fig. 2b, c), which were absent in the cells from liquid culture or the cells adhering on to fluoropolymer-coated steel #2 (Table 2; Figs. 1a, 2g–i).

M. silvanus (Fig. 3b, e) formed giant cells (>10 µm in length) when grown on non-coated (Fig. 3a, b) or DLC-coated (Fig. 3d, e) steels. Many cells showed appendages. Planktonic cells (Fig. 1b) or biofilms on fluoropolymer-coated steel (Fig. 3g–i) expressed neither of the features.

Most cells in *D. geothermalis* biofilms on non-coated (Figs. 4b, c) and DLC-coated steels (Fig. 4d, f) displayed a large number of thin (20 nm) and thick (100 nm) appendages. These thread-shaped organelles in the biofilm connected neighboring cells to one another or to the abiotic surface. The cells grown on fluoropolymer-coated steel displayed only few and only thin appendages (Fig. 4h, i). The planktonic cells (Fig. 1c) were devoid of any thread-like structures.

S. epidermidis grown on non-coated steel (Fig. 5b, c) displayed thick threads bridging neighboring cells to a dense and slimy network. The biofilms of the same strain on DLC- (Fig. 5e, f) or fluoropolymer-coated steel

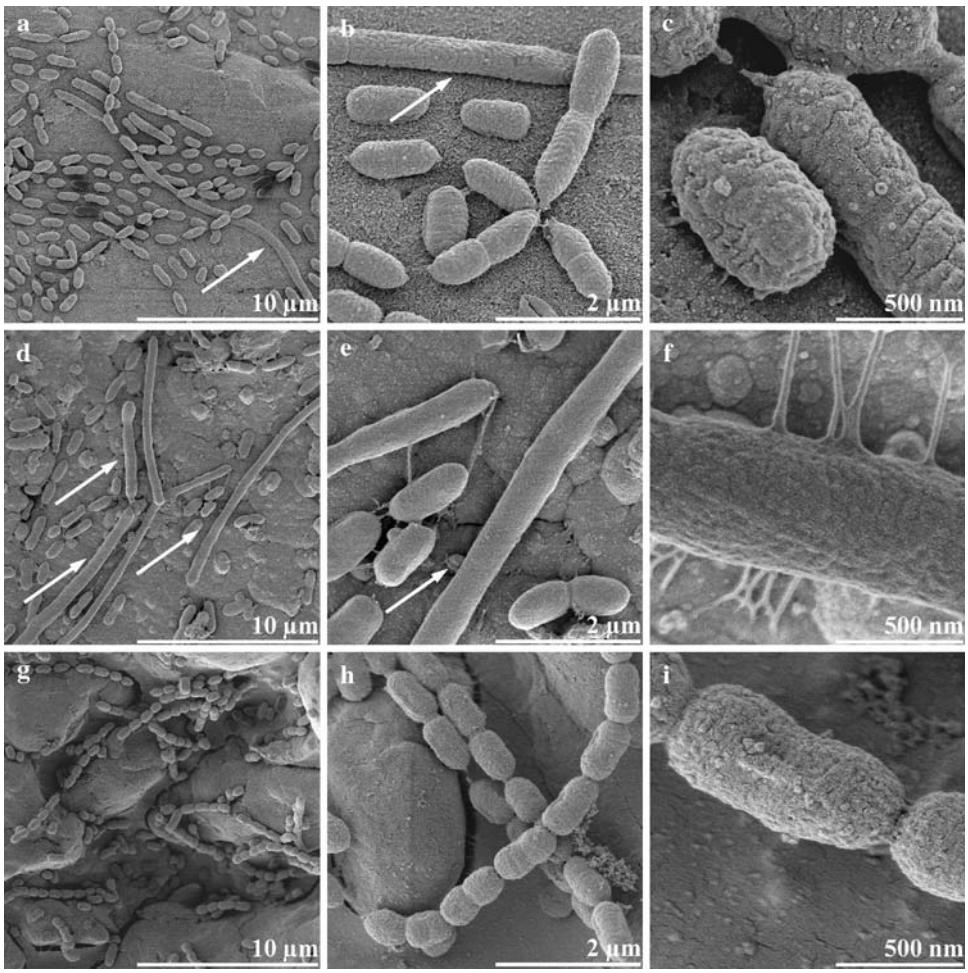

Fig. 3 FESEM micrographs of *M. silvanus* B-R2A5-50.4 adhered to coated or non-coated stainless steels. **a–c** non-coated stainless steel AISI316L/2B (steel #2, Table 2). **d–f** Diamond like carbon coating DLC-A on steel AISI316L/2B. **g–i** AR-115 fluoropolymer-coated acid-fast stainless steel #1.Giant cells (*arrows*) were frequently formed but were not seen in the biofilms formed on the fluoropolymer-coated steel #2

(Fig. 5h, i) consisted of non-slimy cells interconnected by thin appendages only.

Summarizing, the ultrastructures of the four monoculture bacteria were strikingly different depending on whether the bacterium grew in the liquid medium (Fig. 1) or as biofilms (Figs. 2, 3, 4, 5) on the different substrates, indicating interaction between the bacteria and the non-living surfaces. It appears as if coating of the acid proof steel with a fluoropolymer or with a DLC prevented or reduced the formation of the appendages bridging the cells to each other or to the substrate.

The question arises whether this apparent communication between the surface and the adhesion organelles is reflected in the densities of the biofilms. To determine this, biofilms grown on the various coated and non-coated steels were washed to remove loosely adhering cells and the persisting cells were quantitated using fluorochrome staining for nucleic acids (Syto9), which allows estimation of the number of cells. An example of the results obtained for two different non-coated acid proof stainless steels, two DLC coated steels and two fluoropolymer-coated steels is shown in Fig. 6.

Figure 6 shows the quantities of the different biofilm bacteria accumulated on the coated and non-coated steel surfaces, which we denote as adherence. The biofilm density of *Psx. taiwanensis* decreased in the following order: steel #1 > steel #2 > fluoropolymers AR-115, AR-221 > DCL-A, DLC-B. *Staph. epidermidis* biofilm growth had a preference order as follows: steel #1 > fluoropolymers AR-115, AR-221 > steel #2 > DLC-A, DLC-B. Thus both of these test bacteria, a gram-negative gamma-proteobacterium, and gram-positive coccus, were effectively repelled (~70% compared to non-coated steels) by DLC-B and fluoropolymer AR-221 coatings on steel. *M. silvanus* and *D. geothermalis* growth had a preference order as follows: steel #2 > DLC-A, DLC-B, >steel #1 > fluoropolymers AR-115, AR-221. So these two test bacteria were best repelled (up to 90%) by the fluoropolymer coatings on steel. *Psx. taiwanensis* and *Staph. epidermidis* adhered more to steel #1 (coated or non-coated) and *D. geothermalis* and *M. silvanus* to steel #2 (coated or non-coated).

When the results in Fig. 6 are compared to the ultrastructural features shown in Figs. 2, 3, 4, 5, the following can be noted. *Staph. epidermidis* (Fig. 5) formed thick and

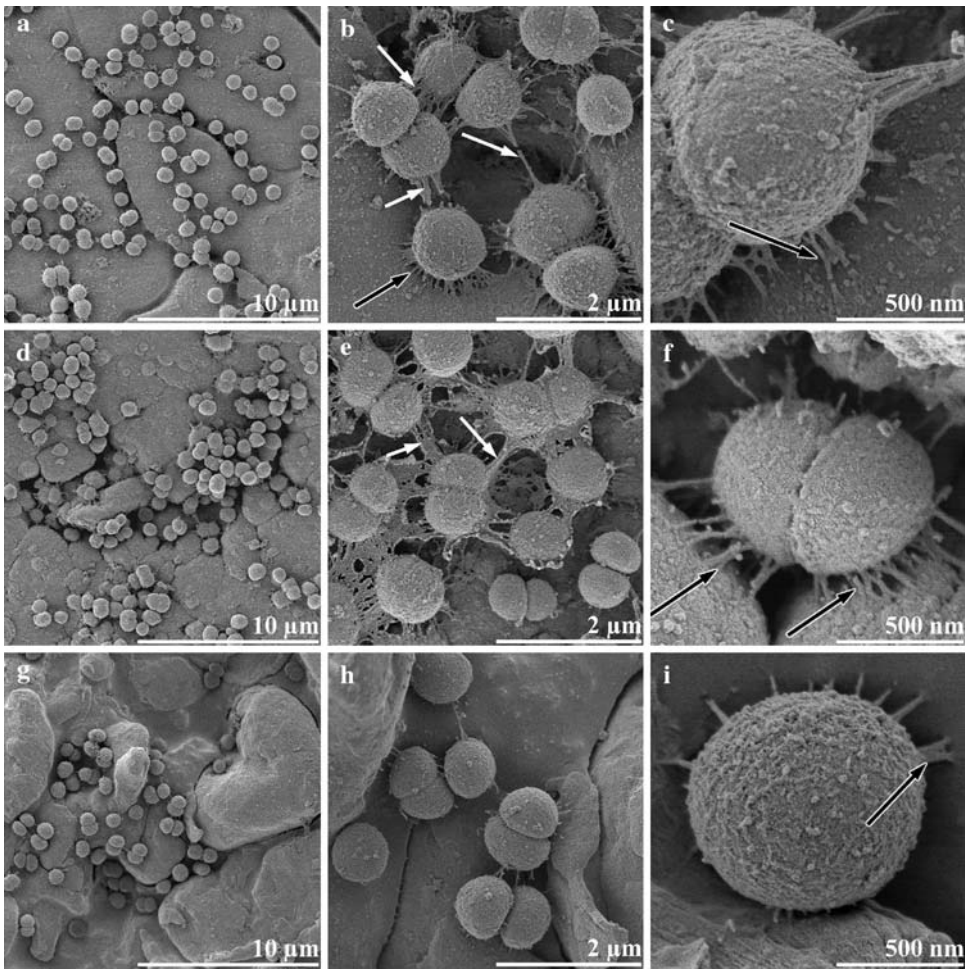

Fig. 4 FESEM micrographs of *D. geothermalis* E50051 adhered to coated and non-coated stainless steels. **a–c** Non-coated stainless steel AISI316L/2B (steel #2, Table 2). **d–f** Diamond like carbon coating DLC-A on steel AISI316L/2B. **g–i** AR-115 fluoropolymer-coated acid-fast stainless steel #1. Micrographs display the threads mediating intercellular adhesion (*white arrows*) and the adhesion threads connecting the cells to the non-living surface (*black arrows*)

numerous adhesion appendages on plain steel. On DLC-coated steel it formed thin, short appendages and were few in number. Similar reduction in the number and the length of adhesion threads was observed for *D. geothermalis* (Fig. 4) and *M silvanus* (Fig. 3) on the fluoropolymer-coated as compared to plain steel. For these three biofilm-forming species, it thus looks like the number/thickness of the adhesion threads in cells growing on the coated/non-coated steels positively correlated with the mass of the accumulating biofilm. In the case of *Psx. taiwanensis,* adhesion threads were visible also on cells grown on the DLC-coated steels (Fig. 2e, f), which nevertheless supported somewhat less accumulation of biofilm than on fluoropolymer-coated steel. The difference was small and in case of *Psx. taiwanensis* the cell ghosts, rather than the adhesion threads, (Fig. 2b, c) may have been the major factor in biofilm adherence onto steel.

The base steels, although both were of acid proof quality and closely similar overall compositions (Table 2), differed in attracting biofilm growth: one (steel #1) attracted *Staph. epidermidis* and *Psx. taiwanensis*, whereas the other (steel #2) was more attractive to *D geothermalis* and *M. silvanus*. To find explanations for the different accumulation of biofilm and the ultrastructural changes of bacteria on coated versus non-coated steel surfaces, energetic properties of the surfaces were measured. Table 3 shows the water contact angles of the test coupons calculated according to the Wenzel equation. Moreover, the work of adhesion of water to surfaces is listed expressing the degree of polarity. The measured contact angles (θ_m) of both fluoropolymer-coated steels in water were, as expected, higher than those of the uncoated steels, corresponding to a reduced water adhesion (hydrophilicity). The apparent higher contact angle of coating AR-115 compared to AR-221 was due to roughness and not to true hydrophobicity, as shown when roughness correction was applied (θ_y). The roughness correction had a significant effect on the contact angle for the AR-115 coating only. The acid proof steel #1 was more hydrophobic than the stainless steel #2. Contents of carbon, chromium and nickel were identical for both steels, but the molybdenum/manganese ratio was higher and silicon content lower in steel #2 as compared to steel #1 (Table 2). However, the θ_m on the coated and non-coated steels #2 were in the range of 80°–90° with standard

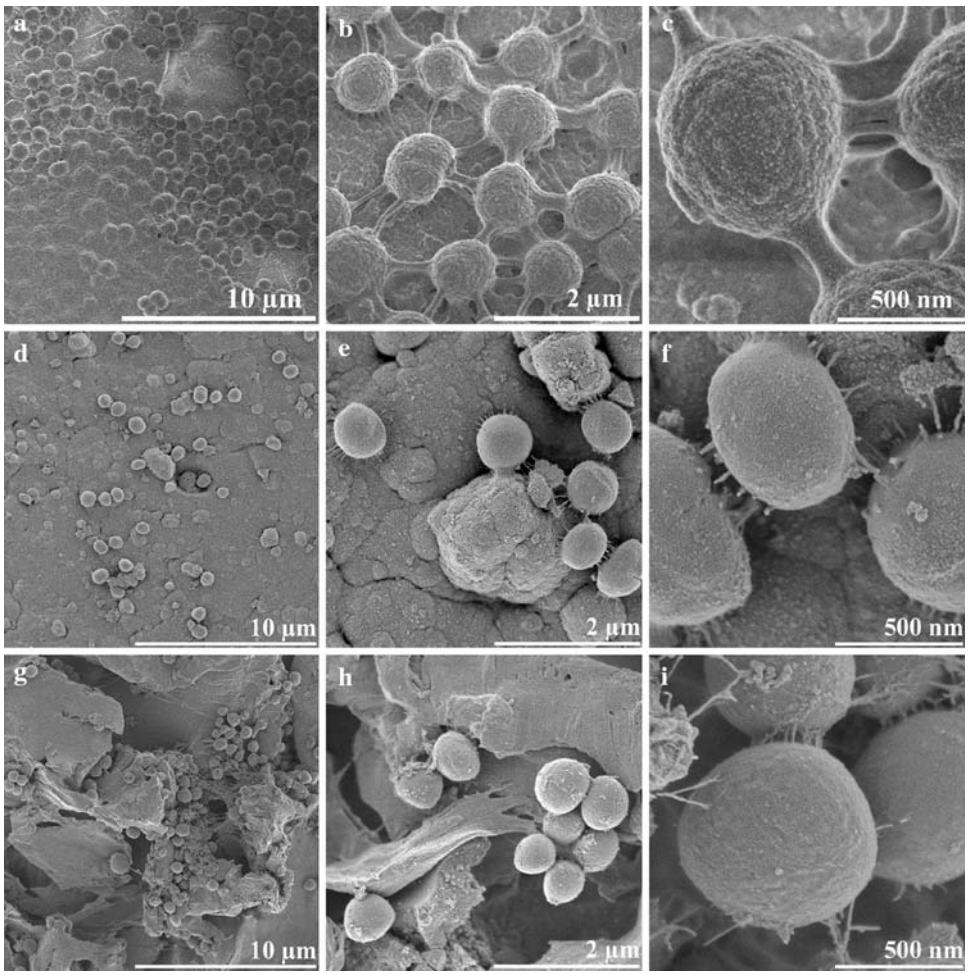

Fig. 5 FESEM micrographs of *Staph. epidermidis* O-47 (PIA+) adhered to coated or non-coated stainless steel surfaces. **a–c** Non-coated stainless steel AISI316L/2B (steel #2, Table 2). **d–f** Diamond like carbon coating DLC-A on steel AISI316L/2B. **g–i** AR-115 fluoropolymer-coated acid-fast stainless steel #1. On steel #2 the biofilm appears slimy (**a**) and adjacent cells are interconnected by thick (100 nm) adhesion threads (**b**, **c**)

deviations up to 10°. This indicates a larger chemical heterogeneity within the steel #2 than steel #1, possibly explaining the different adherence of the biofilm bacteria to these steels (Fig. 6).

When comparing the adherence of different bacterial species with the water adhesion it is seen that *D. geothermalis* and *M. silvanus* adhered most to the highly wetted surfaces, but were largely rejected from the hydrophobic surfaces. *Psx. taiwanensis* and *Staph. epidermidis* adhered on a relative scale less to highly wetting surfaces than to the water-repellent surfaces ($\theta > 90°$). However, on an absolute scale the adherence of *Psx. taiwanensis* exceeds that of *M. silvanus*. Surfaces with low work of adhesion (W_A) in aqueous environment seem to have favored adhesion of *Staph. epidermidis* and *Psx. taiwanensis* indicating that these bacteria behaved in water as hydrophobic particles.

Topographical parameters, measured with AFM, of the test surfaces are compiled in Table 4. For the coated steels, clear differences in the topography were distinguished. Steel #1 with the fluoropolymer-coating AR-115 was very rough (high S_q and S_{dr} values) compared to the relatively smooth fluoropolymer AR-221 coating. Also the differences in skewness (S_{sk}) and kurtosis (S_{ku}) were significant between these coatings. AR-221 had a positive skewness value, indicating lack of surface porosity. The high kurtosis value (as compared to the Gaussian value of 3) of AR-221 shows that the coating included some sharp protrusions. These are factors that may explain the lower attraction of different types of bacteria to AR-221 than to AR-115, in addition to the differences in the work of adhesion. The effect of the DLC-coating thickness on the surface properties of the acid proof steel (steel #2) is reflected in the topographical parameters. The thicker DLC-B coating has a strongly positive skewness value, compared to negative skewness for the non-coated steel and a Gaussian-like value for the DLC-A coating. This might be a reason for the reduction in bacteria adherence to the DLC-B coating compared to the non-coated steel, even though the work of adhesion of water is similar for both surfaces. Similar trends are seen in the kurtosis value.

As overall conclusion, both the surface energy and the topography affected the attraction and the growth of bacteria onto the substrates. *D. geothermalis* and *M. silvanus*

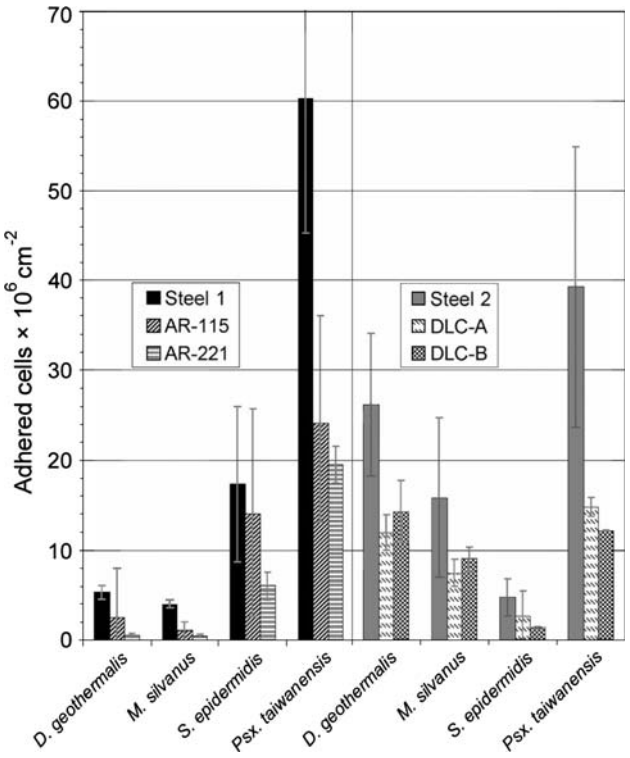

Fig. 6 Adherence of cultures of *D. geothermalis*, *M. silvanus*, *Psx. taiwanensis* and *Staph. epidermidis* onto coated or non-coated stainless steels. Biofilms were grown on the steel coupons immersed in media inoculated with the test strains as described in Table 1. Non-adhered or loosely adhered cells were washed off with water. The coupons were stained with Syto9 and the cell numbers were obtained from the fluorescence readings using a standard curve calibrated by microscopic counting. *Error bars* indicate standard deviations. Stainless steel #1 with fluoropolymer coatings AR-115 (*striped bar*), AR-221 (*horizontal line bar*) or none (*dark shaded bar*). Stainless steel #2 with diamond like carbon coatings DLC-A (*half striped bar*) or DLC-B (*checked bar*) or none (*light shaded bar*)

Table 3 Contact angles measured for non-coated and coated stainless steels

	Mean θ_m^a	SD	r	θ_y^b	W_A (mJ m^{-2})^c
Steel #1	100	1	1.0	99	61.4
AR115	125	1	1.6	111	46.7
AR221	116	1	1.0	115	42.0
Steel #2	79	13	1.1	80	85.4
DLCA	92	8	1.2	91	71.5
DLCB	77	10	1.2	79	86.7

[a] Measured contact angle

[b] Roughness corrected contact angle

[c] W_A (adhesion work) $= \gamma W(\cos\theta + 1)$ using for $\gamma W(20°)$ the value $= 72.8$ mJ m^{-2}

attached easier to hydrophilic surfaces, whereas the opposite took place for *Staph. epidermidis* and *Psx. taiwanensis*. A positive skewness value i.e., a more non-porous surface and decreased the attraction of the test bacteria. High kurtosis values had a similar effect on the adhesion of bacteria.

Discussion

The paper machine biofilm former *D. geothermalis* [18] adheres to glass surfaces by means of adhesion threads, which were only expressed during surface-attached growth [30]. Furthermore, we reported earlier that adhesion thread-like organelles also were involved in adhesion to acid proof steel [27]. In this paper we show that *Staph. epidermidis*, a pathogenic species colonizing medical implants [3, 5, 11] also adhered to acid proof steel with similar kind of adhesion threads as does *D. geothermalis*. The adhesion organelles were also formed in *M. silvanus*, another pink biofilm producer recently identified as major colonizer of paper machines [8]. Thus, the capability to form appendages to adhere to non-living surfaces is not limited to *Deinococcus,* but may be a general phenomenon among cocci as well as rod-shaped bacteria.

This study revealed novel features of cell adhesion and indicated that bacterial adhesiveness could be modified by coating. The ultrastructural analysis of the biofilm-forming species *D. geothermalis, M. silvanus, Staph. epidermidis* and *Psx. taiwanensis* revealed (Fig. 1, 2, 3, 4, 5) that these changed the cell shape as well as the number, length and thickness of the surface exposed appendages in response to the surface they met. The appendages likely represented adhesion tools since they were only expressed on the non-living substrate. There were no adhesion organelles in planktonic cells.

Psx. taiwanensis produces bulky slimes on surfaces of paper machines [4, 19, 36]. The present results indicate that *Psx. taiwanensis* was an extremely efficient biofilm producer on both coated and non-coated stainless steels. The biofilms of this species interestingly consisted more of cell ghosts than viable-looking cells. *Psx. taiwanensis* biofilms depended on suicidal attachment: lysed cells mediated the adhesion of live cells. This kind of a suicidal biofilm generation has not been described earlier, to our knowledge. Another gamma-proteobacterium, *Pseudomonas aeruginosa*, has been shown to generate biofilms with outer membrane vesicles as building blocks [33].

Our results suggest that *D. geothermalis, Staph. epidermidis, Psx. taiwanensis* and *M. silvanus* sensed the surface they were in contact with. This was indicated by ultrastructural changes when the cells attached to differently coated steel surfaces. Contact with non-living substratum possibly liberated signals in the adhered cells, comparable to quorum-sensing behaviour, e.g. for *Serratia marcescens* as reported by Labbate et al. 2007 [21]. The signalling could be species-specific explaining why some species were best repelled by

Table 4 The topographical parameters of non-coated and coated stainless steels. The parameters were measured by atomic force microscopy

	Steel #1						Steel #2					
	Non-coated	SD	AR115	SD	AR221	SD	Non-coated	SD	DLCA	SD	DLCB	SD
S_q (nm)[a]	58.4	11.6	247.8	70.5	32.5	12.3	62.1	16.1	122.0	34.8	93.2	15.7
S_{sk}^b	−0.43	0.39	−0.24	0.40	0.76	0.64	−0.56	0.25	0.17	0.41	0.88	0.50
S_{ku}^c	4.77	1.08	4.40	1.30	7.41	2.79	3.96	0.69	3.17	0.38	7.54	1.17
S_z (nm)[d]	442.3	117.2	1,773.0	435.2	297.5	109.0	456.3	88.8	806.6	208.4	906.9	142.0
S_{ds} (1/μm^2)[e]	27.7	6.5	14.2	3.8	64.3	22.9	37.4	13.5	29.7	3.7	25.7	4.7
S_{dr} (%)[f]	4.0	3.1	61.1	24.4	3.3	0.9	6.4	2.5	15.5	5.0	18.8	3.9

[a] S_q, is the root-mean-square (RMS) roughness, amplitude roughness parameter that gives the standard deviation of height

[b] S_{sk}, surface skewness expresses the asymmetry of the height distribution. A value equal to 0 indicate a Gaussianlike surface, <0 a porous surface (the valleys dominate over the peaks), >0 the local maxima dominating over the valleys

[c] S_{ku}, surface kurtosis the sharpness of the surface height distribution. A Gaussian value for this parameter is 3.0; values $\ll$3.0 indicates a broad height distribution, values $\gg$3.0 refer to almost quantized height values

[d] S_z, ten point height, average of five highest local maxima and five deepest local minima

[e] S_{ds}, number of local maxima per unit area

[f] S_{dr}, the surface area ratio parameter as percent of the projected area

fluoropolymers and others by diamond-like carbon. From the industrial housekeeping point of view, this is unfortunate as it means that biofilm adherence analysis done with one bacterial species does not necessarily predict the biofouling tendency by another species, for example, *Psx. taiwanensis* versus *D. geothermalis.* The DLC coating reduced the accumulation of *Staph. epidermidis* biofilm on steel more efficiently than fluoropolymer coating similarly, as reported by Katsikogianni 2006 [15]. However, the situation was opposite for biofilms of *D. geothermalis* and *M. silvanus*. Thus, the functioning of the coated material for process equipment depends on the microbial species causing the biofilm problem.

We found a new surface property parameter whose positive value indicated low tendency for adhering to each of the four different biofilm-forming test bacteria used in this study: skewness (S_{sk}). High skewness value indicates lack of porosity. In addition, we found that a high value of kurtosis (S_{ku}) indicated decreased tendency of bacterial adhesion. Arnold and Bailey (2000) [2] did not report on these two parameters (S_{sk}, S_{ku}) when they used AFM to assess the effects of topographic parameters on the bacterial adherence to steel.

In the present experimental setup it was found that highly wetting surfaces ($\theta < 90°$) attracted *D. geothermalis* and *M. silvanus,* whereas water-repelling surfaces ($\theta > 90°$) attracted *Psx. taiwanensis* and *Staph. epidermidis*. Our findings prove that bacterial repellence was not determined by surface hydrophobicity alone as anticipated, basing on indirect evidence by Maki et al (1990) [24] and Palmer et al. (2007) [25]. It is possible that the correlations to bacterial adhesiveness would have been different if pH or surface tension were other than that of pure water used for measuring the wettability in this study.

The general trend was that *Staph. epidermidis* and *Psx. taiwanensis* favored hydrophobic surfaces for adhesion in contrast to *D. geothermalis* and *M. silvanus,* which preferably adhered to hydrophilic-coated or non-coated steels. However, this is not the whole truth, as the roughness-corrected contact angle (θ_y) or W_A was not the only factor determining the bacterial adherence to surfaces. A high surface skewness and kurtosis seems also to have a reductive effect on the adherence. *Psx. taivanensis* adhered to both hydrophobic and hydrophilic surfaces and also differed from the other three model bacteria in its adhesion mechanisms involving cell ghosts rather than the thread-like adhesion organelles.

The present study is the first attempt, to our knowledge, to determine properties of the non-living surface important for the adherence of *D. geothermalis*, *Psx. taiwanensis* and *M. silvanus*, representatives of the hot water industrial environment.

Acknowledgments This work was funded as a part of the Technology Programme Clean Surfaces 2002–2006 (PINTA) by the Finnish Funding Agency for Technology and Innovation (Tekes). We also thank the Academy of Finland for the Centre of Excellence grant (53305, MSS), Helsinki University Viikki Science Library for excellent information services, the Faculty of Agriculture and Forestry Instrument Centre for technical support and Leena Steininger, Hannele Tukiainen and Tuula Suortti for many kinds of help.

References

1. Anonymous (2001) In: Anonymous (ed) Image metrology, the scanning probe image processor, SPIP, User's and reference guide. Copenhagen, Denmark
2. Arnold JW, Bailey GW (2000) Surface finishes on stainless steel reduce bacterial attachment and early biofilm formation: scanning

electron and atomic force microscopy study. Poult Sci 79:1839–1845
3. Costerton JW, Montanaro L, Arciola CR (2005) Biofilm in implant infections: its production and regulation. Int J Artif Organs 28:1062–1068
4. Desjardins E, Beaulieu C (2003) Identification of bacteria contaminating pulp and a paper machine in a Canadian paper mill. J Ind Microbiol Biotechnol 30:141–145
5. Donlan RM, Costerton JW (2002) Biofilms: survival mechanisms of clinically relevant microorganisms. Clin Microbiol Rev 15:167–193
6. Dunne WM Jr (2002) Bacterial adhesion: seen any good biofilms lately?. Clin Microbiol Rev 15:155–166
7. Eaton AD, Clesceri LS, Rice EW, Greenberg AE (2005) In: Eaton AD, Clesceri LS, Rice EW and Greenberg AE (eds) Standard methods for the examination of water and wastewater. American Public Health Association, American Water Works Association and Water Environment Federation, Port City Press, Baltimore, Maryland, USA, pp 9-34–9-36
8. Ekman J, Kosonen M, Jokela S, Kolari M, Korhonen P, Salkinoja-Salonen M (2007) Detection and quantitation of colored deposit-forming *Meiothermus* spp. in paper industry processes and end products. J Ind Microbiol Biotechnol 34:203–211
9. Ewald A, Gluckermann SK, Thull R, Gbureck U (2006) Antimicrobial titanium/silver PVD coatings on titanium. Biomed Eng Online 5:22
10. Geesey GG, Bryers JD (2000) Biofouling of engineered materials and systems. In: Bryers JD (ed) Biofilms II: process analysis and applications. Wiley, New York, pp 237–279
11. Götz F (2002) Staphylococcus and biofilms. Mol Microbiol 43:1367–1378
12. Heilmann C, Gerke C, Perdreau-Remington F, Götz F (1996) Characterization of Tn917 insertion mutants of Staphylococcus epidermidis affected in biofilm formation. Infect Immun 64:277–282
13. Johnson JR, Kuskowski MA, Wilt TJ (2006) Systematic review: antimicrobial urinary catheters to prevent catheter-associated urinary tract infection in hospitalized patients. Ann Intern Med 144:116–126
14. Kalyon BD, Olgun U (2001) Antibacterial efficacy of triclosan-incorporated polymers. See comment. Am J Infect Control 29:124–125
15. Katsikogianni M, Spiliopoulou I, Dowling DP, Missirlis YF (2006) Adhesion of slime producing Staphylococcus epidermidis strains to PVC and diamond-like carbon/silver/fluorinated coatings. J Mater Sci Mater Med 17:679–689
16. Klueh U, Wagner V, Kelly S, Johnson A, Bryers JD (2000) Efficacy of silver-coated fabric to prevent bacterial colonization and subsequent device-based biofilm formation. J Biomed Mater Res 53:621–631
17. Kolari M (2003) Attachment mechanisms and properties of bacterial biofilms on non-living surfaces. Dissertationes Biocentri Viikki Universitatis Helsingiensis 12/2003, PhD Thesis University of Helsinki, Department of Applied Chemistry and Microbiology, Helsinki, Finland
18. Kolari M, Nuutinen J, Rainey FA, Salkinoja-Salonen MS (2003) Colored moderately thermophilic bacteria in paper-machine biofilms. J Ind Microbiol Biotechnol 30:225–238
19. Kuosmanen T, Peltola M, Raulio M, Pulliainen M, Laurila T, Selin J-, Huopalainen H, Salkinoja-Salonen MS (2006) Effect of polarization on manganese biofouling of heat exchanger surfaces. In: Müller-Steinhagen H, Malayeri MR, Watkinson AP (eds) Proceedings of the 6th international conference on heat exchangers fouling and cleaning—challenges and opportunities. Engineering Conferences International, ECI Symposium Series, http://services.bepress.com/eci/heatexchanger2005/41/. RP2. 41, pp 283–288
20. Kwok CS, Wan C, Hendricks S, Bryers JD, Horbett TA, Ratner BD (1999) Design of infection-resistant antibiotic-releasing polymers: I. Fabrication and formulation. J Control Release 62:289–299
21. Labbate M, Zhu H, Thung L, Bandara R, Larsen MR, Willcox MD, Givskov M, Rice SA, Kjelleberg S (2007) Quorum-sensing regulation of adhesion in Serratia marcescens MG1 is surface dependent. J Bacteriol 189:2702–2711
22. Li C, Zhang X, Whitbourne R (1999) In vitro antimicrobial activity of a new antiseptic central venous catheter. J Biomater Appl 13:206–223
23. Mack D, Rohde H, Harris LG, Davies AP, Horstkotte MA, Knobloch JK (2006) Biofilm formation in medical device-related infection. Int J Artif Organs 29:343–359
24. Maki JS, Little BJ, Wagner P, Mitchell R (1990) Biofilm formation on metal surface in Antarctic waters. Biofouling 2:27–38
25. Palmer J, Flint S, Brooks J (2007) Bacterial cell attachment, the beginning of a biofilm. J Ind Microbiol Biotechnol 34:577–588
26. Peltonen J, Jarn M, Areva S, Linden M, Rosenholm JB (2004) Topographical parameters for specifying a three-dimensional surface. Langmuir 20:9428–9431
27. Raulio M, Pore V, Areva S, Ritala M, Leskela M, Linden M, Rosenholm JB, Lounatmaa K, Salkinoja-Salonen M (2006) Destruction of Deinococcus geothermalis biofilm by photocatalytic ALD and sol-gel TiO(2) surfaces. J Ind Microbiol Biotechnol 33:261–268
28. Rees EN, Tebbs SE, Elliott TS (1998) Role of antimicrobial-impregnated polymer and Teflon in the prevention of biliary stent blockage. J Hosp Infect 39:323–329
29. Rupp ME, Fey PD, Heilmann C, Götz F (2001) Characterization of the importance of Staphylococcus epidermidis autolysin and polysaccharide intercellular adhesin in the pathogenesis of intravascular catheter-associated infection in a rat model. J Infect Dis 183:1038–1042
30. Saarimaa C, Peltola M, Raulio M, Neu TR, Salkinoja-Salonen MS, Neubauer P (2006) Characterization of adhesion threads of Deinococcus geothermalis as Type IV Pili. J Bacteriol 188:7016–7021
31. Schierholz JM, Lucas LJ, Rump A, Pulverer G (1998) Efficacy of silver-coated medical devices. J Hosp Infect 40:257–262
32. Schierholz JM, Steinhauser H, Rump AF, Berkels R, Pulverer G (1997) Controlled release of antibiotics from biomedical polyurethanes: morphological and structural features. Biomaterials 18:839–844
33. Schooling SR, Beveridge TJ (2006) Membrane vesicles: an overlooked component of the matrices of biofilms. J Bacteriol 188:5945–5957
34. Söderquist B (2007) Surgical site infections in cardiac surgery: microbiology. APMIS 115:1008–1011
35. Stout KJ, Sullivan PJ, Dong WP, Mainsah E, Luo N, Mathia T, Zahouani H (1994) The development of methods for the characterization of roughness on three dimensions
36. Suihko ML, Sinkko H, Partanen L, Mattila-Sandholm T, Salkinoja-Salonen M, Raaska L (2004) Description of heterotrophic bacteria occurring in paper mills and paper products. J Appl Microbiol 97:1228–1235
37. Väisänen OM, Weber A, Bennasar A, Rainey FA, Busse HJ, Salkinoja-Salonen MS (1998) Microbial communities of printing paper machines. J Appl Microbiol 84:1069–1084
38. van de Belt H, Neut D, Schenk W, van Horn JR, van Der Mei HC, Busscher HJ (2001) Staphylococcus aureus biofilm formation on different gentamicin-loaded polymethylmethacrylate bone cements. Biomaterials 22:1607–1611
39. Wenzel RN (1936) Resistance of solid surfaces to wetting by water. Ind Eng Chem 28:988–994